

# A solid-state $^{13}\text{C}$ NMR analysis of molecular dynamics in aramide polymers

Dan McElheny<sup>a</sup>, Veronica Frydman<sup>b</sup>, Lucio Frydman<sup>b,\*</sup>

<sup>a</sup>*Division of Biological Sciences, University of Chicago, Chicago, IL 60637, USA*

<sup>b</sup>*Faculty of Chemistry, Weizmann Institute of Sciences, 76100 Rehovot, Israel*

Received 22 May 2005; received in revised form 8 August 2005

Available online 30 September 2005

Dedicated to Alex Pines in celebration of his 60th birthday

## Abstract

The local dynamics of aromatic cores was analyzed for a homologous series of polyamides in the solid phase incorporating phenyl, biphenyl and naphthyl groups. Preliminary wide-line and spin-relaxation variable-temperature  $^1\text{H}$  NMR measurements revealed the presence of thermally activated molecular motions for each polymer studied. A number of  $^{13}\text{C}$  NMR experiments were then implemented to further clarify the nature and extent of such motions. These included  $^1\text{H}$ – $^{13}\text{C}$  2D separate-local-field measurements, whose line shapes revealed that motions involved for all cases a superposition of states. These could in principle be associated with rigid and mobile populations in these semi-crystalline aramides, a model that yielded a proper description of the spectra at all temperatures. To further probe this model the relaxation behavior of the aramides'  $^{13}\text{C}$  spins was monitored in the rotating frame as a function of temperature, in both the presence and absence of homonuclear  $^1\text{H}$ – $^1\text{H}$  decoupling. The variations observed in these measurements evidenced a thermally activated, relatively broad distribution of motional rates in the polymers. Editing the 2D local-field data according to the  $^{13}\text{C}$  relaxation also supported this heterogeneous dynamic model. The mechanism underlying this behavior and implications towards the  $^{13}\text{C}$  analysis of motions in aramides in particular and complex polymers in general, is briefly discussed.

© 2005 Elsevier Inc. All rights reserved.

**Keywords:** Dynamics and spin relaxation

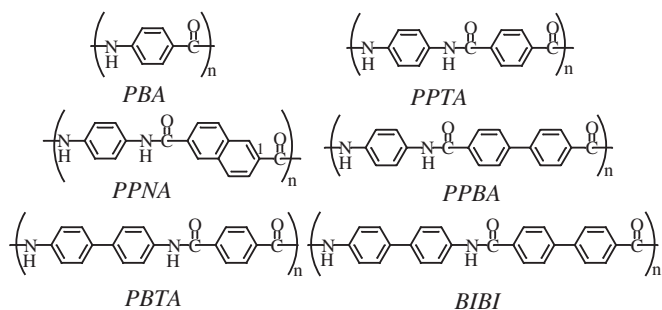
## 1. Introduction

The molecular dynamics of polymers in general and liquid crystalline polymers in particular, is known to deeply affect the tensile and impact properties of these materials [1,2]. Extensive efforts have been devoted to define the dynamic/mechanical relationships in such semi-crystalline macromolecules via a variety of means, of which NMR provides one of the most detailed molecular probes [3–5]. In this contribution we employ an assortment of natural abundance solid-state NMR techniques in order to study dynamics within the homologous series of aromatic polyamide (aramide) polymers illustrated in Scheme 1. The interest in the molecular dynamics of these liquid

crystalline polymers reflects the fact that such ultra-strong materials are utilized in the solid state [2,6,7]. The main constituent within this family of polymers is poly (*p*-phenylene)-terephthalamide (PPTA), which upon being spun from a liquid-crystalline solution serves as the basis for the Kevlar<sup>®</sup> brand of commercial fibers [8–10]. PPTA fibers have been analyzed by a wide variety of analytical techniques including solid-state NMR [11–16], and been shown to possess both crystalline and amorphous portions which exhibit significantly different dynamic behaviors. This kind of dynamic heterogeneity is best elucidated if a number of complementary spectroscopic approaches are used to measure the rates of motion encountered. We describe here the application of a variety of solid-state dynamic NMR approaches to the elucidation of motions in aramides, and make a critical evaluation of the potential and limitations encountered when applying such natural

\*Corresponding author. Fax: +972 8 9344123.

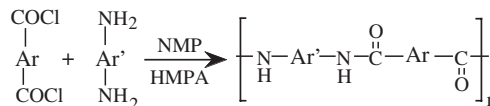
E-mail address: [lucio.frydman@weizmann.ac.il](mailto:lucio.frydman@weizmann.ac.il) (L. Frydman).



Scheme 1.

abundance NMR experiments to this kind of heterogeneous systems.

NMR has traditionally been used to analyze solid-state dynamics by relying on relaxation rate measurements, on line shape changes, and on multi-dimensional exchange correlations [3–5,17,18]. Each of these approaches is sensitive to dynamics over a particular range of timescales, defined by both the technique as well as by the type of interaction being monitored. For example measurements of spin-lattice relaxation  $T_1$  are sensitive to correlation times  $\tau_c \approx \omega_0^{-1} \leq 10^{-7}$  s, motions which are considered fast in solid-state environments. An intermediate dynamic regime with correlation times between  $10^{-7}$  s  $< \tau_c < 10^{-3}$  s can be monitored either through line shape changes from the dipolar or chemical shift anisotropies, or through rotating-frame relaxation ( $T_{1\rho}$ ) measurements. The slowest of molecular dynamic processes can usually be followed with multi-dimensional exchange NMR measurements, which monitor correlation times up to the  $T_1$  times of the nuclei being studied (in the order of seconds). As part of the present study we decided to focus on the first two of these regimes, in the hope of better defining the wide range of thermal processes potentially arising in aramides. Our main observable stemmed from fitting the line shape changes arising in aromatic  $^1\text{H}$ – $^{13}\text{C}$  dipolar field spectra. Such line shapes are readily discerned in so-called two-dimensional separate-local-field magic-angle-spinning (2D SLF MAS) NMR [19–23], a family of techniques capable of revealing as sideband spectra the extent of the dynamics occurring for each isotropic site in a molecule. In the present work such data were measured and analyzed to extract information about the types of motions that might be occurring within the homologous aramide polymer series in Scheme 1. In an effort to better define the actual kinetic rates of the motions detected by the 2D SLF MAS NMR data, relaxation studies were also implemented. It was concluded that in the simplest of these sequences, involving  $T_{1\rho}$  measurements, the processes driving the temperature-dependent spin relaxation did not arise solely from the molecular motions revealed by the SLF data. Because spin relaxation is widely used for quantitatively analyzing the rates of polymer dynamics, we considered it worthwhile contrasting the different pictures provided by the SLF and



Scheme 2.

the  $T_{1\rho}$  relaxation data for each polymer. Further conclusions regarding aramide dynamics in particular and dynamic NMR in general, are described below.

## 2. Experimental

All the determinations described in the present study were carried out on polymer samples synthesized in our laboratory following guidelines described in patented procedures [24,25]. The main feature of these preparations are summarized in Scheme 2. All NMR measurements were carried out using laboratory-built multiple-resonance NMR spectrometers; the majority utilizing a 7.2 T Magnex magnet equipped with a commercial 4 mm Varian/Che-magnetics Pencil probe and variable-temperature accessories, and the remainder on a 11.75 T solids apparatus. For the 1D and 2D  $^{13}\text{C}$  NMR acquisitions we used a ramped cross polarization centered at  $\approx 50$  kHz,  $^1\text{H}$  decoupling at  $\approx 100$  kHz, and MAS at 10 kHz. Details for the specific kind of 2D SLF MAS acquisitions utilized in the present work, both in terms of their experimental setup, their processing and analysis, have been extensively discussed in Ref. [26].

## 3. Results and discussion

### 3.1. Dynamic dipolar line shape changes in aramides

Before attempting to quantify the potentially complex molecular dynamics occurring in the aramide series through 2D  $^{13}\text{C}$  NMR experiments, we found it advantageous to test the overall presence of such dynamics via the acquisition of static  $^1\text{H}$  NMR spectra. This in turn provides a simple and sensitivity route for probing molecular dynamics in the systems of interest, while yielding an approximate value of the point at which motions at rates comparable to the  $^1\text{H}$  dipolar line width ( $\approx 50$  kHz) activate [17,18]. Fig. 1 illustrates static 501 MHz  $^1\text{H}$  NMR spectra recorded for the aramides, over a fairly wide ( $>400^\circ\text{C}$ ) temperature range. The spectral changes observed are quite pronounced, attesting to the presence of dynamics in all members of the aramide family. Moreover, the dynamics seem to affect the  $^1\text{H}$  line widths in a nearly continuous fashion as a function of temperature. This is by contrast to the more step-like changes usually found in molecular crystals, and is suggestive of a distribution of kinetic rates.

Having unambiguously defined the presence of molecular motions in the aramides' solid state, variable-temperature

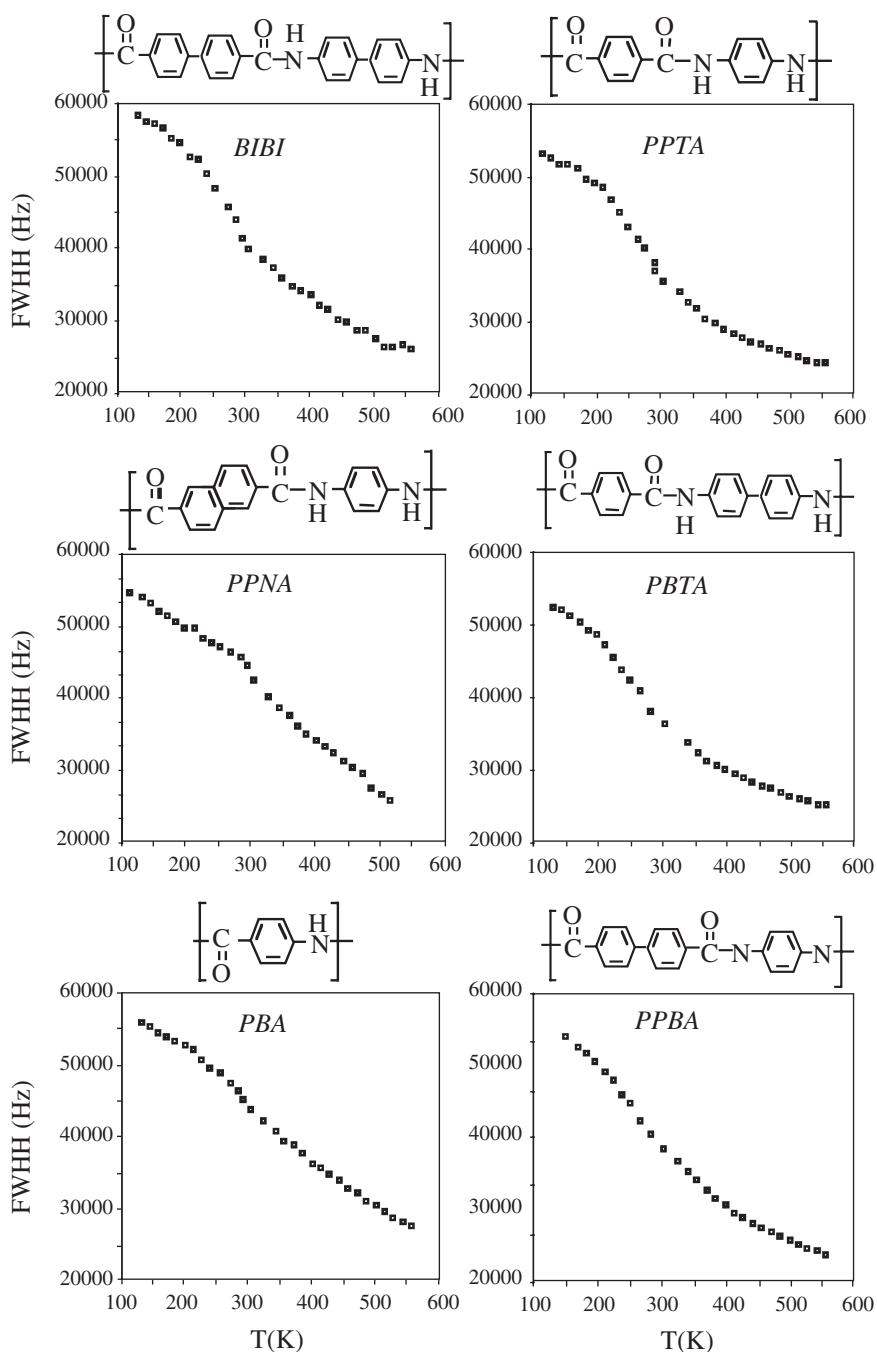


Fig. 1. Temperature dependencies observed for the static proton NMR half-height line widths (FWHH) for each of the indicated polymer structures. All these line width changes were found to be entirely reversible, and are ascribed to the onset of thermally activated local motions.

2D SLF MAS NMR methods were applied onto them. When compared with the  $^1\text{H}$  wide-line data the SLF method possesses significant advantages, providing a local atomic-site resolution as well as actual line shapes susceptible to analysis on the basis of dynamics models. Representative  $^1\text{H}$ - $^{13}\text{C}$  local field MAS NMR spectra extracted for individual chemical sites from the various polymers studied in this series are shown in Fig. 2, for a range of chosen temperatures. In accordance with the  $^1\text{H}$  wide-line results, one can appreciate that for all polymers the sideband

intensities vary with temperature, indicating the onset of local motions. Yet a more careful analysis of the temperature dependence reveals that each individual type of aromatic ring within each different polymer, exhibits a slightly different dynamic behavior. For example, judging from the sideband intensities, the spectrum of PBA exhibits at the lowest temperature ( $-60^\circ\text{C}$ ) a static-like  $^1\text{H}$ - $^{13}\text{C}$  interaction of 24.5 kHz. Essentially all dynamic processes for this polymer are consequently frozen (vis-à-vis the relevant NMR timescale) at this temperature. As the temperature

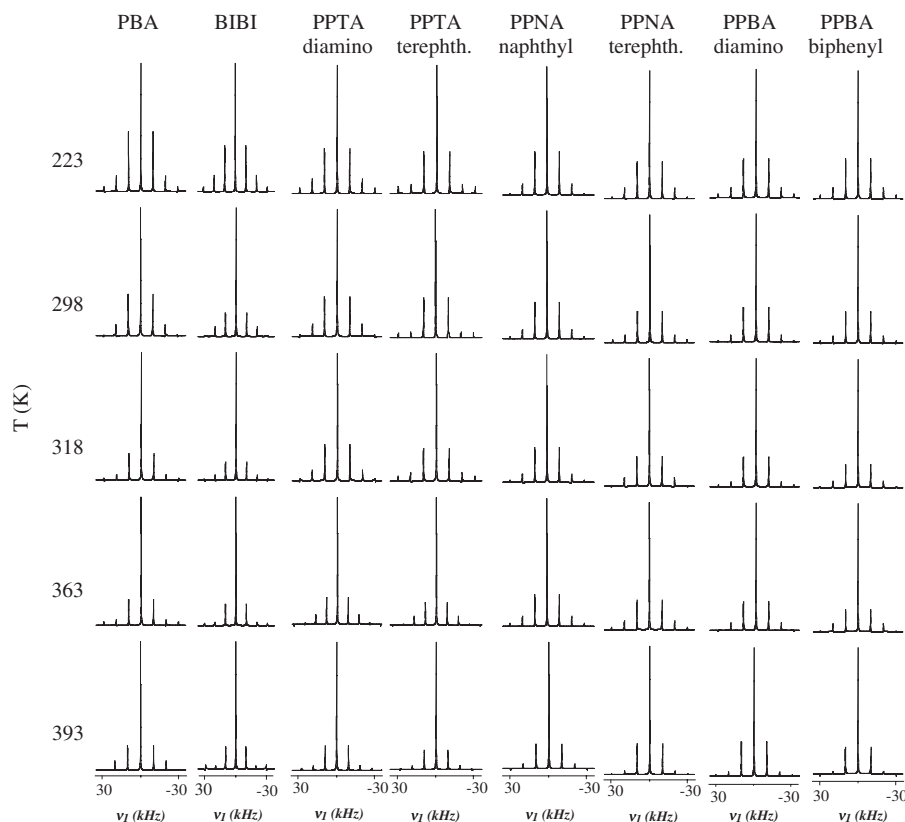


Fig. 2.  $^1\text{H}$ – $^{13}\text{C}$  SLF dipolar line shapes recorded as a function of temperature for the polyaramide family. The traces were extracted from 2D experiments carried out at 7.2 T (75.8 MHz  $^{13}\text{C}$  Larmor frequency) as described in Ref. [26], using no amplification of the heteronuclear dipolar couplings and MAS at 10.0 kHz. Note that dipolar spectra correspond to specific sites of the indicated polymers (e.g., diamino, terephthalic, biphenyl, or naphthyl rings), chosen by selecting the appropriate carbon resonance along the orthogonal dimension.

rises the sideband intensities begin to drop with respect to the centerband, yet they never disappear completely as would be the case for a rapidly flipping free-rotor type of ring motion [5,26]. In fact the dynamic changes shown by PBA's SLF spectra cannot be simulated at all temperatures by assuming that a single kind of dynamic behavior characterizes the whole sample: spectral interpretation requires assuming at least two dynamically distinct kinds of populations, whose relative ratio changes with temperature. For instance a very good fit arises if it is assumed that the sample is made up from static and  $\pi$ -flipping ring populations (Fig. 3); a similarly good fit—both for PBA as well as the for the remaining polymers in the series—can also be achieved by superimposing populations of static and of librating aromatic rings<sup>1</sup>. As a matter of fact, a dynamic librational model has been put forward for rationalizing the static  $^2\text{H}$  NMR line shapes observed for specifically deuterated analogs of PPTA. Once again, static line shapes had to be superimposed here onto librational averaged ones in order to reproduce, via simulations, the changes

experimentally observed by deuterium NMR [12,13]. Yet considering all the  $^1\text{H}$ – $^{13}\text{C}$  local field data in unison, we feel inclined to adopt a  $\pi$ -flipping rather than a librational model in order to account for the progressive dynamic averaging shown in Fig. 2. Indeed for most of the aramides—and for the biphenyl (BIBI) polymer in particular—the SLF MAS NMR spectra stabilize past a given temperature in line shapes that match the sideband patterns expected for  $\pi$ -flipping motions. Upon further heating these samples no additional averaging is apparent, a behavior suggestive of a constrained motion rather than of diffusive-like librations. And while this does not serve as a proof that a well-defined two-site motion is responsible for all the averaging observed (as mentioned, simulations based on static and librational populations could also reproduce the experimental data) we decided to interpret all our experimental sideband spectra on the basis of temperature-dependent static +  $\pi$ -flipping aromatic ring populations.

Using this dynamic model as starting point for a discussion, Fig. 4 plots the percentage of  $\pi$ -flipping rings resulting from the various SLF MAS analyses carried out on different aramides, when repeated as a function of sample temperature. As can be seen most aramides have at least one ring displaying a substantial mobility, even down to  $-60^\circ\text{C}$ . Only PBA reveals an essentially static material

<sup>1</sup>This ambiguity arises from the fact that when oscillating over a well spanning  $\approx 65^\circ$ , the SLF MAS line shapes arising from such freely-rotating librators become essentially indistinguishable for those arising from a fast  $\pi$ -flipping motion.

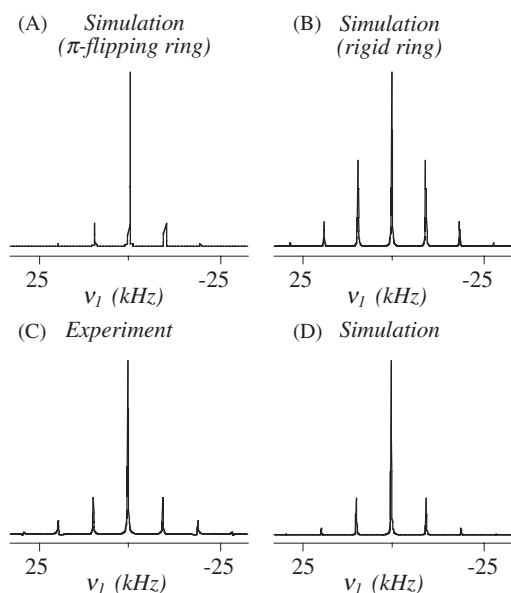


Fig. 3. Principles of the static/dynamic population analysis used to model the SLF NMR data. Shown on top are the spectral simulations for an isolated C–H pair assuming that: (A) aromatic rings execute  $\pi$ -flips about their *para* axes; (B) the aromatic rings are rigid. Both sets assumed MAS at 10 kHz and a standard phenyl ring geometry (1.07 Å proton–carbon internuclear distance and 120° bond angles). Shown at the bottom is the actual spectral analysis for the case of a PBA  $^{13}\text{C}$  resonance: (C) SLF trace acquired at 90 °C with a 10 kHz spinning rate; (D) best fit simulation found upon superimposing a  $\pi$ -flipping population of 62% and a rigid-ring population of 38%. All simulations throughout this work were calculated using custom written programs, which integrated the Bloch equations of motions for isolated  $^{13}\text{C}$ - $^1\text{H}$  spin pairs undergoing MAS at all orientations within a rotor, and then subjecting the resulting time-domain set to Fourier transform [5,27].

at this temperature, perhaps an indication of the more efficient and homogeneous packing that can be achieved by this polymer. Also the naphthyl-based PPNA polymer shows a distinct behavior in that the change in its dynamic populations is not very substantial as a function of temperature. The distinctive features observed for these two polymer are also picked up by  $^1\text{H}$  relaxation measurement (vide infra).

Lastly, it is worth comparing in further detail our results against previous deuterium NMR studies on PPTA [12,13,28]. PPTA is thought of as being a highly crystalline material with an idealized structure consisting of radially stacked hydrogen-bonded sheets of molecules, further organized into a pleated sheet structure nearly parallel to the long molecular axis [29,30]. Although this X-ray diffraction model of PPTA incorporates no amorphous character into the material, transmission electron microscopy [31] along with the deuterium NMR studies (as well as the SLF results of this work) reveal a heterogeneous and dynamic structure. It has been argued that this bimodal heterogeneity stems from the crystallite's surfaces having substantially different dynamics than their interiors. And indeed, if the fraction of PPTA's flipping rings is plotted as a function of inverse temperature, two different dynamic

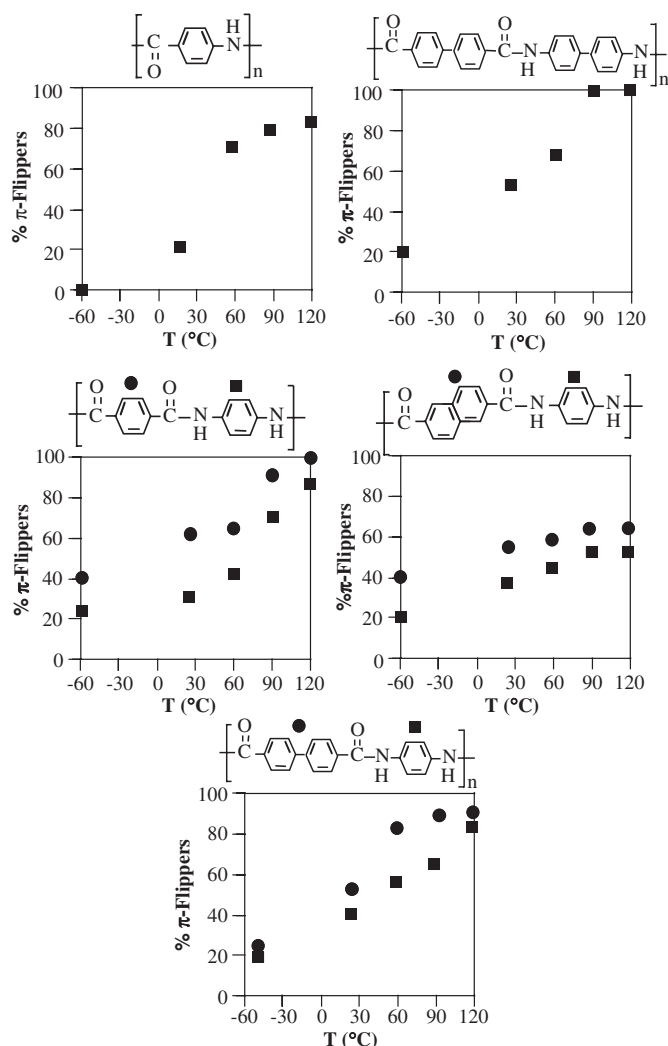


Fig. 4. Percentage of  $\pi$ -flipping rings extracted for the indicated aramide polymer sites as a function of temperature (for monomers containing more than one chemically discernible ring, individual sites are indicated by squares and circles). Quantification of these data entailed simulations of the experimental SLF sideband patterns, taking into account different relative contributions from the rigid and flipping ring populations as described in Fig. 3.

regimes seem evident both for the diamino as well as the terephthaloyl rings (Fig. 5). For the diamino ring there is even good quantitative agreement between the  $^{13}\text{C}$  local field data and the 'librator-fraction' detected by  $^2\text{H}$  NMR for PPTA (dashed lines in Fig. 5, top). Such behavior, however, could also be reflecting a stretched exponential activation profile, liable to be present in such heterogeneous systems. An interesting difference between the previous deuterium NMR results and our natural abundance studies is the higher fraction of dynamic rings that we consistently detect. This could perhaps be reflecting the slightly slower motions that aromatic rings experience upon  $^1\text{H}/^2\text{H}$  substitution; NMR studies have suggested that slight changes in bond lengths such as those introduced by isotopic labels, could have substantial effects

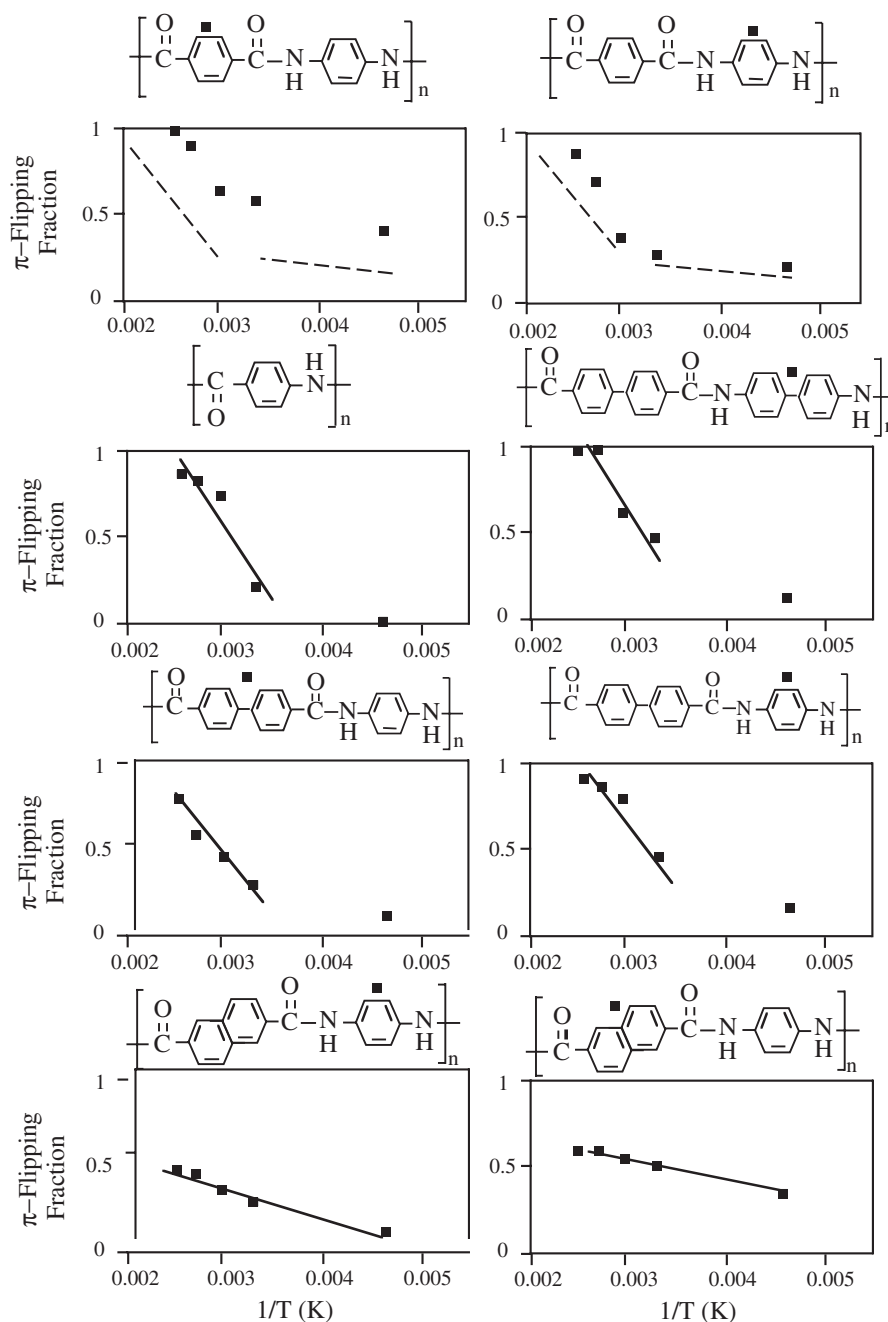


Fig. 5. Similar plots as described in Fig. 4, but displayed as a function of reciprocal temperatures. These plots convey information about the energetics of the ring motions.

on the ability of aromatic rings to flip [32]. Also interesting to note is the fact that most other aramide polymers also seem to have a bimodal activation behavior similar to the one exhibited by PPTA. The sole exception is once again PPNA, which has a dynamically homogeneous dependence of  $\pi$ -flippers as a function of inverse temperature.

### 3.2. Aramide dynamics: information available from spin relaxation

The previous paragraph illustrates some of the insight that natural abundance SLF NMR methods can provide

about aramide motions at a local level. And yet, although the resulting line shapes could afford the relative populations of static and flipping aromatic rings within the polymers, these measurements are by themselves unable to quantify the absolute rates of these dynamics. Indeed SLF protocols act very much like ‘lowpass filters’, cataloguing motions as either slow or fast with respect to a relevant NMR timescale given in this case by the  $^1\text{H}$ – $^{13}\text{C}$  heteronuclear dipolar interaction. But they cannot pinpoint the actual rate distributions characterizing such motions. In order to extract this kinetic insight we set out to implement complementary experimental NMR measurements, which

could potentially quantify the rates of the molecular dynamics. A well-established approach for determining absolute rates and kinetic activation energies of molecules in solids involves measuring the system's longitudinal spin relaxation, both in the laboratory and in the rotating frames of reference [17,18]. The corresponding relaxation times  $T_1$  and  $T_{1\rho}$  are sensitive reporters on the dynamics of molecules occurring within the neighborhood of the corresponding frequencies  $\gamma B_0$  and  $\gamma B_1$ ; as these nutation rates span the 10–100 MHz and 10–100 kHz ranges, respectively, they serve to characterize fast and intermediate motions such as those typically occurring in crystalline or amorphous solids.

As a starting point to evaluate the spectral range characterizing motions in aramides, we began by measuring the  $^1\text{H}$  longitudinal relaxation times for the various polymers.  $T_1$ 's resulting from fitting inversion-recovery experiments acquired as a function of temperature, are given in Fig. 6. The general behavior observed for most polymers is similar, with relaxation times being on the order of 1–10 s while showing only a gradual change (usually less than an order of magnitude) as temperature of several hundreds of degrees. This is typical of systems characterized by ultra-slow molecular motions, whose rates are far from the Larmor frequency of operation at all but the highest temperatures. The only exception to such behavior is once again furnished by PPNA, which has

significantly shorter relaxation times than the remaining aramides. Yet interpreting the molecular origin of this difference solely on the basis of dynamics is complicated by the fact that a number of explanations could be invoked to rationalize the short relaxation time ( $T_1 \leq 1$  s) observed for this polymer at even the lowest of temperatures.

Apart from this PPNA instance, the  $^1\text{H}$   $T_1$  results for all polymers are consistent with the onset of the slow, thermally activated motion processes revealed in Figs. 1 and 2. Having collected these  $^1\text{H}$  and  $^1\text{H}$ - $^{13}\text{C}$  NMR data we know that these are all macrocyclic-related dynamics occurring in the neighborhood of 1–100 kHz at ambient temperatures. It is generally accepted that such a timescale regime can be appropriately studied by measuring relaxation in the rotating frame,  $T_{1\rho}$ , which monitors the exchange of energies between the spins and the lattice in the presence of a spin-locking field  $\nu_1 = \gamma B_1 \approx 10 - 100$  kHz. Rather than measuring  $T_{1\rho}$  relaxation times on protons we decided to focus on gathering high-resolution relaxation data from  $^{13}\text{C}$  MAS NMR, as such measurements would be characterized by a much higher chemical site specificity. Shown in Fig. 7 is a representative set of aramide rotating frame relaxation data obtained from the typical  $^{13}\text{C}$   $T_{1\rho}$ -measuring pulse sequence, showing magnetization decay curves observed for the diamino ring carbons of PPTA as a function of temperature at a spin-lock field  $\nu_1 = 40$  kHz. At first sight such data (as well as those collected for all other polymer) look very promising, because their decay seem to exhibit the kind of biexponential behavior reflecting the co-existence of

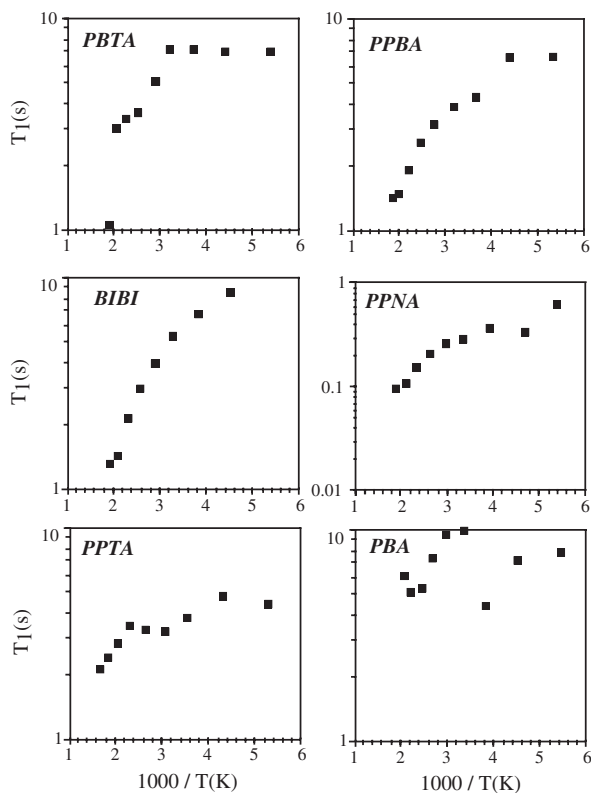


Fig. 6. Proton  $T_1$  times measured for the indicated polymers as a function of temperature. Conventional inversion-recovery sequences were implemented at 302 MHz in these static-sample experiments, leading to a single exponential behavior from which relaxation times were extracted.

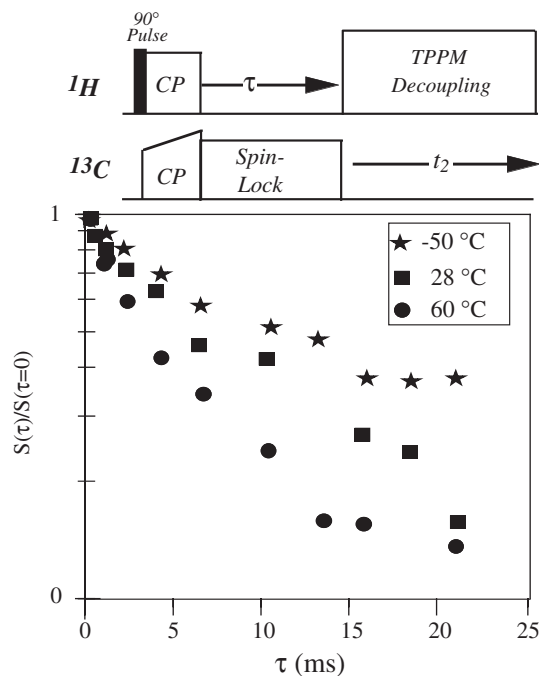


Fig. 7.  $^{13}\text{C}$  magnetization decay curves obtained for PPTA's diamino ring with a 40 kHz spin-locking field as a function of temperature. Experiments were carried out at 7.2 T while undergoing 10 kHz MAS utilizing the sequence on top. Note the apparent biexponentiality of the resulting decays, as well as the shortening of the relaxation time with increasing temperatures.

a dynamic and of a static population. Indeed, this is the behavior that could have been adumbrated from the 2D SLF MAS NMR results. The  $T_{1\rho}$  data also seem to have the proper thermal dependence, since as temperature is raised the growth of the ring-flipping population would explain the progressively faster decays exhibited in Fig. 7. However, when attempting to fit these data with biexponential functions associated to putative dynamic and static populations, we were generally unable to obtain even a semi-quantitative agreement with the populations derived from the SLF MAS NMR data. In fact for all polymers the dynamic populations extracted from this kind of decay curves were consistently far too high, and upon closer inspection they were found to yield  $T_{1\rho}$  times that were simply too short for what could be considered as mobile regions in the samples. Given the proven reliability of the SLF data when dealing with motions in aromatic rings, this finding casts doubts on the usefulness of standard  $T_{1\rho}$  measurements of the kind summarized in Fig. 7 as a proper tool for extracting quantitative insight on the nature of heterogeneous dynamics. Motivated by this we decided to apply such measurements on a model compound known to be crystalline and devoid of dynamic heterogeneities; we turn next to a brief digression on such experiments on this model sample.

Crystalline L-Alanine was chosen as a test model, as it should display essentially a single-crystallite-like relaxation behavior characterized with relatively long relaxation times. Yet as illustrated in Fig. 8A for this molecule's  $C_\alpha$  site, the spin-lock behavior at  $\nu_1 = 40$  kHz shows a short relaxation time and even a somewhat biexponential  $T_{1\rho}$  decay reminiscent of that evidenced by the aramides. An explanation for this behavior was put forward in the literature [33–35], where it was demonstrated that not only molecular motions but also  $^1\text{H}$ – $^1\text{H}$  spin-diffusion processes can contribute via their field fluctuations to define the  $T_{1\rho}$

relaxation of  $^{13}\text{C}$  sites. The timescale of such proton fluctuations will be in the order of the dipolar line width of the  $^1\text{H}$  NMR signal, and hence most influential at the spin-locking rates usually accessed during  $^{13}\text{C}$   $T_{1\rho}$  measurements. Furthermore,  $^1\text{H}$  dipolar line widths (and hence the rates of  $^1\text{H}$ – $^1\text{H}$  spin-diffusion) can also be expected to show a temperature dependence upon the onset of dynamics, thereby complicating the derivation of kinetic conclusions solely on the basis of temperature changes. A possible route to deal with such spin-diffusion complications, is to take the  $^{13}\text{C}$  spin-locking field away as far as possible from the  $^1\text{H}$ – $^1\text{H}$  dipolar spin-diffusion timescale. And indeed as the rates of the  $^{13}\text{C}$  spin-lock become higher (Fig. 8B), the rotating frame decay of the  $C_\alpha$  magnetization becomes considerably slower as well as nearly single-exponential. Still, in an effort to overcome spin-diffusion effects completely, a different approach based on the Lee–Goldburg (LG) experiment was assayed. In this form of  $T_{1\rho}$  experiment an off-resonance LG decoupling field applied to the protons, will scale  $^{13}\text{C}$ – $^1\text{H}$  couplings while achieving complete  $^1\text{H}$ – $^1\text{H}$  decoupling by setting the spin-space  $^1\text{H}$  magnetization axis at the magic angle condition [36]. In order to minimize dipolar recoupling effects related to cross polarization, the  $^1\text{H}$  decoupling fields were set to three times that of the spin-locking field [37]; no significant differences on the  $^{13}\text{C}$  relaxation were observed upon changing this LG decoupling to a fast frequency-switched version [38], and thus the use of such FSLG irradiation wasn't pursued. In any case, upon accurately setting the spin-space magic-angle condition (by varying the  $^1\text{H}$  irradiation offset—see inset in Fig. 8C), the resulting LG- $T_{1\rho}$   $^{13}\text{C}_\alpha$  relaxation time ended up an order of magnitude longer than in the original experiment (Fig. 8). This difference highlights the complications that homonuclear proton spin-diffusion processes may introduce on the analysis of heteronuclear data, if not suitably accounted

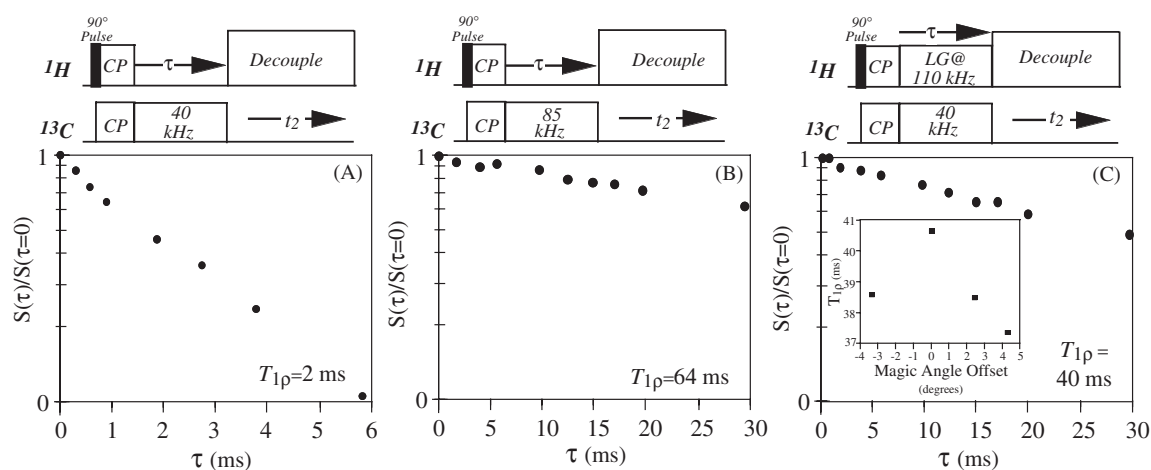


Fig. 8. Various rotating frame  $^{13}\text{C}$  NMR relaxation rate measurement strategies and their corresponding results, when applied to a polycrystalline sample of L-Alanine undergoing MAS. The nutation fields employed in each of the rf channels are included in the pulse sequences at the top of each experimental data set; other details are as in Fig. 7. In the Lee–Goldburg  $T_{1\rho}$  experiment (C), an effective  $^1\text{H}$  nutation rate of 110 kHz was achieved by combining an appropriate off-resonance offset with  $\nu_1 = 64$  kHz. The inset illustrates the  $^1\text{H}$ -offset dependence (translated into degrees off the magic axis) observed for the  $^{13}\text{C}$  relaxation time in the neighborhood of the optimum LG condition.

for by  $^1\text{H}$ – $^1\text{H}$  decoupling, by intense spin-locking fields, or preferably by a combination of thereof (always while keeping clear from potential  $^{13}\text{C}$ – $^1\text{H}$  cross-polarization processes).

In view of the relaxation behavior observed for Alanine,  $^{13}\text{C}$  LG- $T_{1\rho}$  experiments were also undertaken on the aramide systems. As expected, the results obtained were then considerably different from those observed in the conventional  $^{13}\text{C}$   $T_{1\rho}$  measurements. A representative instance of this is shown in Fig. 9 for the case of PPTA, whose  $^{13}\text{C}$  relaxation times still exhibit a temperature dependence but without evidencing the strong biexponential behavior displayed by the earlier relaxation curves (Fig. 7). In fact the relaxation data obtained both in this manner as well as using the high-power variant in Fig. 8B, could for all polymers be fitted with a single exponential curve with a quality that was comparable to that of a biexponential fit. This was to some extent unexpected—perhaps even disappointing—given the partitioning between mobile and rigid populations that had been evidenced by the 2D SLF MAS data. And yet we believe that both kinds of spectral characterizations are valid, and together they reflect the dynamics that characterize the solid aramides. Indeed all experiments reveal that these solid materials entail a dynamic distribution. This heterogeneity places a limit on the ability of spin-relaxation measurements to furnish a detailed description of the kinetics, since for all the temperature and/or spin-locking fields that could be accessed the decaying curves will always detect superpositions of a range of faster and slower decaying exponentials. This in turn will smear away any evidence of biexponential behavior, and prevent any single portion of the  $^{13}\text{C}$  decay curve to be associated with either

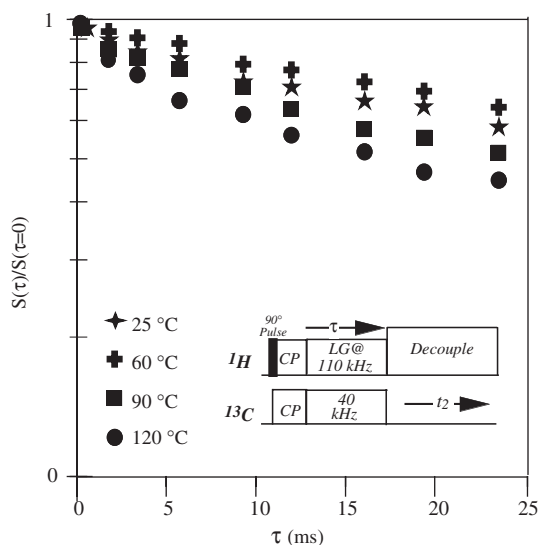


Fig. 9.  $^{13}\text{C}$  rotating-frame relaxation behavior observed for PPTA's diamino ring as a function of temperature. Under the employed  $^1\text{H}$  LG decoupling conditions no strong biexponential behavior is observed, and the average relaxation  $T_{1\rho}$ 's are considerably longer than in the absence of  $^1\text{H}$  irradiation (cf. Fig. 7) at every temperature.

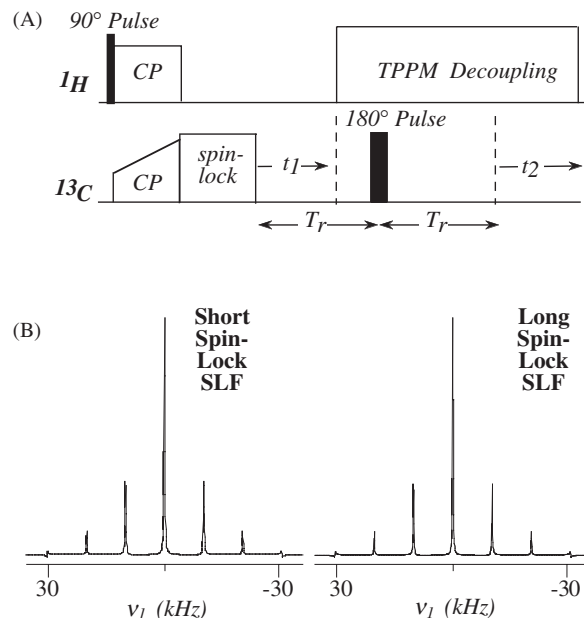


Fig. 10. (A) Pulse sequence utilized to test the dependence of SLF MAS NMR patterns on the  $^{13}\text{C}$   $T_{1\rho}$  parameters. (B) Comparison between the heteronuclear dipolar spectra arising from PPTA's diamino ring sites at room temperature, upon utilizing a  $^{13}\text{C}$  spin-locking field as short as  $100\ \mu\text{s}$  (left) and going all the way up to 4 ms (right). Notice the similarity between both spectral sets.

purely mobile or purely static polymer regions. Perhaps a more graphical evidence for this interpretation is illustrated in Fig. 10, which shows  $^1\text{H}$ – $^{13}\text{C}$  SLF MAS NMR spectra recorded from PPTA's diamino ring after inserting both a short and a long spin-lock periods prior to allowing for the  $^1\text{H}$ – $^{13}\text{C}$  dipolar evolution. Notice that the MAS sideband intensities arising in these two experiments are essentially indistinguishable, suggesting that the heteronuclear SLF MAS spectroscopy detects identical motional character of the  $^{13}\text{C}$  sites regardless of whether probing the initial or latter parts of their spin relaxation curve.

#### 4. Conclusions

A variety of NMR experiments were applied towards the elucidation of dynamic properties in a homologous series of aramide materials. First and foremost among these was 2D SLF MAS NMR at natural abundance, whose simplicity enabled us to extend previous deuterium NMR results on PPTA to a larger variety of polymers. The most relevant conclusion of these experiments is the overall similarity of the dynamics shown by all the aramides, both in terms of their microscopic nature as well as in terms of their overall thermal activation parameters. Indeed minor differences were observed among the spectra and in their temperature dependencies; yet in all cases the motions included a superposition of static and dynamics populations, where aromatic rings became substantially mobile past room temperature. A quantitative line shape analysis

of these SLF data suggested a  $\pi$ -flipping of the rings as most likely for the motions. When careful ancillary relaxation measurements were carried out to quantify the dynamic rates of such motions, the complexity and heterogeneity of the aramides' kinetics became fully evidenced. Also re-discovered in this process were the risks associated to an over-interpretation of  $^{13}\text{C}$   $T_{1\rho}$  relaxation measurements carried out under the influence of  $^1\text{H}$ – $^1\text{H}$  spin-diffusion. Further experimental observables (based for instance on multi-dimensional exchange and distance constraint methods) should probably be developed, in order to enable a better definition of the dynamics in such heterogeneous systems. In fact it is likely that only by relying on a combination of strategies—each one probing a different geometric and kinetic aspect of the dynamics—may characterizations in complex polymer or biopolymers systems (such as the aramides) achieve a realistic description of all the ongoing kinetic events.

### Acknowledgments

This research was supported in part by the Philip M. Klutznick and Ilse Katz Research Funds (Weizmann Institute), and by the Minerva Foundation.

### References

- [1] N.G. McCrum, B.E. Read, G. Williams, *Anelastic and Dielectric Effects in Polymeric Solids*, Wiley, London, 1967.
- [2] M. Gordon, H. Cantou, (Eds.), *Adv. Polym. Sci.* 59–61 (1984).
- [3] H.W. Spiess, *Chem. Rev.* 91 (1991) 1321.
- [4] V.J. McBrierty, K.J. Packer, *Nuclear Magnetic Resonance in Solid Polymers*, Cambridge University Press, Cambridge, 1993.
- [5] K. Schmidt-Rohr, H.W. Spiess, *Multidimensional Solid-State NMR and Polymers*, Academic Press, New York, 1994.
- [6] C. Carfagna (Ed.), *Liquid Crystalline Polymers*, Pergamon Press, Oxford, 1994.
- [7] A.I. Isayev, T. Kyu, S.Z.D. Cheng (Eds.), *Liquid Crystalline Polymer Systems*, ACS Press, Washington, 1996.
- [8] S.L. Kwolek, P.W. Morgan, J.R. Schaeffgen, L.W. Gulrich, *Macromolecules* 10 (1977) 1390.
- [9] T.I. Bair, P.W. Morgan, F.L. Killian, *Macromolecules* 10 (1977) 1396.
- [10] H.H. Yang, *Aromatic High-Strength Fibers*, Wiley, New York, 1989.
- [11] A.D. English, *J. Polym. Sci.: Polym. Phys. Ed.* 24 (1986) 805.
- [12] R.J. Schadt, K.H. Gardner, V. Gabara, S.R. Allen, D.B. Chase, A.D. English, *Macromolecules* 26 (1993) 6509.
- [13] R.J. Schadt, E.J. Cain, K.H. Gardner, V. Gabara, S.R. Allen, A.D. English, *Macromolecules* 28 (1995) 1152.
- [14] J. Hong, G.S. Harbison, *Polym. Prepr.* 31 (1990) 115.
- [15] M. Wilhelm, S.F.D. Lacroix, J.J. Titman, K. Schmidt-Rohr, H.W. Spiess, *Acta Polym.* 44 (1993) 279.
- [16] J.R. Sachleben, L. Frydman, *Solid State NMR* 7 (1997) 301.
- [17] M. Mehring, *High Resolution NMR in Solids*, Springer, Berlin, 1983.
- [18] C.A. Fyfe, *Solid State NMR for Chemists*, CFC Press, Ontario, 1983.
- [19] M.G. Munowitz, R.G. Griffin, G. Bodenhausen, T.H. Wang, *J. Am. Chem. Soc.* 103 (1981) 2529.
- [20] M.G. Munowitz, R.G. Griffin, *J. Chem. Phys.* 76 (1982) 2848.
- [21] J. Schaefer, R.A. McKay, E.O. Stejskal, W.T. Dixon, *J. Magn. Reson.* 52 (1983) 123.
- [22] J. Schaefer, E.O. Stejskal, R.A. McKay, W.T. Dixon, *Macromolecules* 17 (1984) 1479.
- [23] J.E. Roberts, G.S. Harbison, M.G. Munowitz, J. Herzfeld, R.G. Griffin, *J. Am. Chem. Soc.* 109 (1987) 4163.
- [24] S.L. Kwolek, US Patent 3,671,542, June 20, 1972.
- [25] S.L. Kwolek, US Patent 3,819,582, June 25, 1974.
- [26] D. McElheny, E. DeVita, L. Frydman, *J. Magn. Reson.* 143 (2000) 321.
- [27] M.M. Maricq, J.S. Waugh, *J. Chem. Phys.* 70 (1979) 3300.
- [28] R.J. Schadt, E.J. Cain, K.H. Gardner, V. Gabara, S.R. Allen, A.D. English, *Polym. Prepr.* 32 (1991) 253.
- [29] M.G. Northolt, *Eur. Polym. J.* 10 (1974) 799.
- [30] M.G. Dobb, D.J. Johnson, B.P. Saville, *J. Polym. Sci. Polym. Phys. Ed.* 15 (1977) 2201.
- [31] C.L. Jackson, R.J. Schadt, K.H. Gardner, D.B. Chase, S.R. Allen, V. Gabara, A.D. English, *Polymer* 54 (1993) 233.
- [32] M.P. Espe, B.R. Mattes, J. Schaefer, *Macromolecules* 30 (1997) 6312.
- [33] D.L. VanderHart, A.N. Garroway, *J. Chem. Phys.* 71 (1979) 2773.
- [34] J. Schaefer, M.D. Sefcik, E.O. Stejskal, R.A. McKay, *Macromolecules* 14 (1981) 280.
- [35] W. Garielse, G.H. Angad, F.C. Feyen, W.S. Veeman, *Macromolecules* 27 (1994) 5811.
- [36] M. Lee, W.I. Goldburg, *Phys. Rev. A* 410 (1965) 1261.
- [37] Y. Ishii, J. Ashida, T. Terao, *Chem. Phys. Lett.* 246 (1995) 439.
- [38] A. Bielecki, A.C. Kolber, H.J.M. deGroot, R.G. Griffin, M.H. Levitt, *Adv. Magn. Reson.* 14 (1990) 111.